● RESEARCH ARTICLE

Extracellular matrix from human umbilical cord-derived mesenchymal stem cells as a scaffold for peripheral nerve regeneration

Bo Xiao[1, 2, 3, #], Feng Rao[4, #], Zhi-yuan Guo[5], Xun Sun[1, 2], Yi-guo Wang[1, 2], Shu-yun Liu[1, 2], Ai-yuan Wang[1, 2], Quan-yi Guo[1, 2], Hao-ye Meng[1, 2], Qing Zhao[1, 3], Jiang Peng[1, 3], Yu Wang[1, 3, *], Shi-bi Lu[1, 2, *]

1 Institute of Orthopedics, Chinese PLA General Hospital, Beijing, China
2 Beijing Key Laboratory of Regenerative Medicine in Orthopedics, Beijing, China
3 The Neural Regeneration Co-innovation Center of Jiangsu Province, Nantong, Jiangsu Province, China
4 Department of Orthopedics, First Affiliated Hospital, School of Medicine, Shihezi University, Shihezi, Xinjiang Uygur Autonomous Region, China
5 Department of Orthopedics, Cangzhou Central Hospital, Cangzhou, Hebei Province, China

Graphical Abstract

Extracellular matrix from human umbilical cord-derived mesenchymal stem cells provides an ideal niche for peripheral nerve regeneration
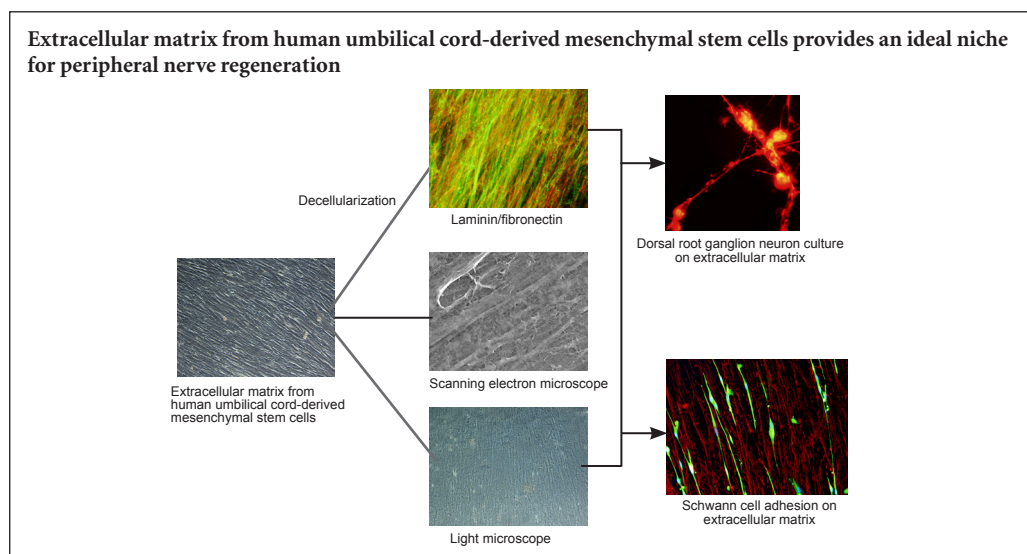
Correspondence to:
Yu Wang, Ph.D. or Shi-bi Lu, M.D.,
wangwangdian628@126.com or
shibilu94@163.com

#These authors contributed equally to this study.

orcid:
0000-0001-7811-5834
(Yu Wang)
0000-0001-5333-4061
(Shi-bi Lu)

Abstract

The extracellular matrix, which includes collagens, laminin, or fibronectin, plays an important role in peripheral nerve regeneration. Recently, a Schwann cell-derived extracellular matrix with classical biomaterial was used to mimic the neural niche. However, extensive clinical use of Schwann cells remains limited because of the limited origin, loss of an autologous nerve, and extended *in vitro* culture times. In the present study, human umbilical cord-derived mesenchymal stem cells (hUCMSCs), which are easily accessible and more proliferative than Schwann cells, were used to prepare an extracellular matrix. We identified the morphology and function of hUCMSCs and investigated their effect on peripheral nerve regeneration. Compared with a non-coated dish tissue culture, the hUCMSC-derived extracellular matrix enhanced Schwann cell proliferation, upregulated gene and protein expression levels of brain-derived neurotrophic factor, glial cell-derived neurotrophic factor, and vascular endothelial growth factor in Schwann cells, and enhanced neurite outgrowth from dorsal root ganglion neurons. These findings suggest that the hUCMSC-derived extracellular matrix promotes peripheral nerve repair and can be used as a basis for the rational design of engineered neural niches.

Key Words: nerve regeneration; peripheral nerve regeneration; mesenchymal stem cells; extracellular matrix; Schwann cell; dorsal root ganglion neuron; niche; neurotropic factors; collagen; laminin; fibronectin; neural regeneration

Introduction

The extracellular matrix (ECM) is an integrated physiological matrix comprising a series of molecules, including proteins, glycoproteins, proteoglycans, and non-proteoglycan polysaccharides secreted by cells within the tissues (Gonzalez-Perez et al., 2013). ECMs have been shown to regulate cell adhesion, proliferation, migration, differentiation, and interactions, and ECMs also provide a structural support (Plantman, 2013). Moreover, ECMs sustain an appropriate microenvironment for tissue regeneration (Gould, 2016). In the peripheral nerve system, the ECM is found in the endoneurium and basal lamina, arranged around axon-Schwann cell (SC) units and mainly composed of laminin, fibronectin, and collagen I and IV (Byron et al., 2013; Gao et al., 2013). After injury, the ECM is secreted by invading fibroblasts and dedifferentiated SCs, which sequentially form collagen fibrils and basal lamina tubes that bridge the nerve gap. Subsequently, renewed axons grow through the nerve gap along the new ECM scaffold (Brown et al., 2009). Taken together, these results suggest that the ECM plays an important role in peripheral nerve regeneration.

To mimic the native microenvironment of peripheral nerve regeneration, individual ECM molecules, including laminin, fibronectin, collagen, and fibrin, were used in various *in vitro* and *in vivo* models (Chen and Strickland, 2003; Armstrong et al., 2007; Yu et al., 2009). Unfortunately, individual ECM molecules fail to build an ideal niche, because different ECM molecules play a role in different functions, and any individual molecule cannot substitute for the entire ECM. Subsequently, a tissue-derived ECM was used for peripheral nerve repair, consisting of decellularized ECM derived from allogeneic or xenogenic tissue. Compared with individual ECM molecules, tissue-derived ECM can preserve a majority of ECM components of the native nerve. However, tissue-derived ECM has several disadvantages, including limited donors and the potential for inflammatory reactions, graft-versus-host disease, pathogen transfer, and uncontrollable degradation (Wang et al., 2012).

In contrast, cell-derived ECM obtained from cultured cells may help to resolve the above-mentioned issues with tissue-derived ECM, because it can be cultured and expanded under pathogen-free conditions to prevent pathogen transfer (Zhang et al., 2016). Recently, SC-derived ECM with classical biomaterials was used to mimic the neural niche (Gu et al., 2014). However, extensive clinical use of SCs remains limited because of the limited origin, loss of an autologous nerve, and extensive *in vitro* culture times. In the present study, we evaluated ECM derived from human umbilical cord-derived mesenchymal stem cells (hUCMSCs), which are more easily accessible and have greater proliferative and secretory abilities than SCs. Compared with adult stem cells, fetal stem cell-derived ECM, which is considered a young ECM, easily enhances cell differentiation and generates more ECM molecules. However, the application of hUCMSC-derived ECM has not been established for peripheral nerve regeneration (Hoshiba et al., 2016).

Our study developed a protocol to establish and characterize hUCMSC-derived ECM, and examined the effects of hUCMSC-derived ECM on SC properties and neurite outgrowth from dorsal root ganglion (DRG) neurons.

Materials and Methods

Animals

Forty 3-day-old Sprague-Dawley rats and six 12-hour-old Sprague-Dawley rats were purchased from the Laboratory Animal Center of the Academy of Military Medical Sciences, Beijing, China (SCXK-military-2012-0004). All rats were housed under specific pathogen-free conditions before the day of each experiment. The 3-day-old rats were used to culture primary Schwann cells, and the 12-hour-old rats were used to culture dorsal root ganglion neurons. The study protocol was approved by the Ethics Committee of the Chinese PLA General Hospital, China. All efforts were made to minimize the number of rats used and their suffering. All procedures were implemented in accordance with the Guide for the Care and Use of Laboratory Animals.

hUCMSC culture and identification

For hUCMSC culture, 12 human umbilical cords were obtained from healthy parturients, who provided informed consent. The procedure was approved by the Institutional Ethics Committee of the Chinese PLA General Hospital in China.

hUCMSCs were isolated and cultured as previously described (Peng et al., 2011). Briefly, after rinsing with phosphate-buffered saline (PBS; Sigma, St. Louis, MO, USA), samples were cut into small pieces (2–3 cm), and cord vessels (two arteries and one vein) and amnion were removed. The Wharton's jelly tissue was then excised, minced into pieces (0.5–1.0 cm^3), placed directly into 75-cm^2 plastic flasks for culture expansion in minimum essential medium-α (Gibco) containing 10% fetal bovine serum (Gibco) and 100 U/mL penicillin/streptomycin (Sigma), and incubated at 37°C in a 5% CO_2 incubator. After reaching 80% confluency, cells were resuspended with 0.25% trypsin-ethylenediamine tetraacetic acid (Corning) and seeded into new culture flasks.

To identify the multidifferentiation capacity of stem cells, passage 2 (P2) hUCMSCs were treated with three types of induction medium – osteogenic, adipogenic, and chondrogenic medium – for 21 days as previously described (Peng et al., 2011). After the induction procedure, cells were stained with Alizarin red, Oil-red O, and Alcian blue to label osteoblasts, adipocytes, and chondrocytes, respectively.

Single-cell suspensions were washed three times in PBS, quantified, and adjusted to the appropriate concentrations. The cells (10^6 per sample) were separately incubated with anti-CD34-FITC, anti-CD44-APC, anti-CD73-APC, anti-CD90-FITC, anti-CD105-PE, and anti-CD45-PerCP antibodies (1:1,000; BD Pharmingen, San Diego, CA, USA). An isotype antibody was used as the control group. The ImageStreamx Mark II (Merck Millipore, Germany) was used to analyze the hUCMSC phenotype.

hUCMSC-derived ECM formation

hUCMSCs (2×10^5 cells/10 cm^2) at P4 were cultured on

the surface of glass carriers precoated with fibronectin (25 μg/mL, Sigma) for 1 hour in 6-well plates. The cells were first cultured in the standard culture medium described above for 3 days until confluent. The cells were continually cultured in fresh maintenance medium supplemented with ascorbic acid (50 mM; Sigma) for 7–9 days to stimulate ECM formation. The medium was routinely changed every 3–4 days during the entire procedure. For decellularization, cells were removed as previously described (Chen et al., 2007; Prewitz et al., 2013). Briefly, samples were washed with PBS at 37°C for 10 minutes and then dried at room temperature, followed by successive treatments with 0.5% (v/v) Triton X-100 (Sigma) plus 20 mM NH_4OH (Sigma) in PBS for 5 minutes at 37°C and with DNase (100 U/mL; Sigma) for 1 hour at 37°C. After washing three times with PBS, the hUCMSC-derived ECM was stored in PBS containing 100 U/mL penicillin/streptomycin (Sigma) at 4°C.

Scanning electron microscopy

The ECM samples were washed three times with PBS and fixed with 2.5% glutaraldehyde for 30 minutes. The samples were then dehydrated twice in gradient concentrations of ethanol (from 30% to 100%) for 10 minutes, followed by replacement of ethanol with tertiary butanol (from 50% to 100%), and finally, lyophilized using a vacuum drier. After samples were coated with gold using a JEOL JFC-110E Ion Sputter, they were observed under a Zeiss MERLIN scanning electron microscope (Oberkochen, Germany).

Immunohistochemical staining

The ECM sample was fixed with 4% paraformaldehyde for 15 minutes at room temperature, washed with PBS, and blocked with 5% normal goat serum (Gibco) for 1 hour. The samples were incubated with the relevant primary antibodies in 2% goat serum overnight at 4°C: rabbit polyclonal antibody against laminin (1:200; Abcam, Cambridge, UK), mouse monoclonal antibody against fibronectin (1:200; Abcam), mouse monoclonal antibody against collagen I (1:200; Abcam), rabbit polyclonal antibody against collagen IV (1:200; Abcam), and mouse monoclonal antibody against collagen X (1:500; Abcam). Nonspecific isotype IgG was used as a negative control. After washing with PBS, samples were incubated with the appropriate fluorescent-labeled secondary antibodies for 1 hour in the dark: Alexa Fluor® 488 donkey anti-rabbit IgG (1:100; Invitrogen, Carlsbad, CA, USA), Alexa Fluor® 594 donkey anti-rabbit IgG (1:100; Invitrogen), Alexa Fluor® 488 donkey anti-mouse IgG (1:100; Invitrogen), and Alexa Fluor® 594 donkey anti-mouse IgG (1:100; Invitrogen). Images were collected under fluorescence microscopy (Olympus Imaging Systems, Tokyo, Japan).

SC culture

Primary SCs were cultured as previously described (Gu et al., 2012). Briefly, sciatic nerves were harvested from Sprague-Dawley rats (1–3 days old), minced into pieces, and enzymatically digested in 0.2% collagenase NB4 (Serva, Heidelberg, Germany) for 10 minutes. After pellets were dis-

sociated by pipetting up and down with a glass pipette, the mixture was centrifuged and resuspended in DMEM/F12 supplemented with 10% fetal bovine serum and then seeded into culture flasks. In the first 24 hours, 10 mM cytosine arabinoside was used to remove the fibroblasts, and was then replaced with growth medium containing 10% fetal bovine serum, heregulin-β-1 (10 ng/mL), forskolin (2 mM), penicillin (100 U/mL), and streptomycin (100 μg/mL). When the cells were 90% confluent, they were trypsinized, centrifuged, resuspended, and plated onto non-coated (control group) or ECM-coated dishes (ECM group) at a cell density of $3 \times 10^4/cm^2$.

5-Ethynyl-2′ -deoxyuridine (EdU)/Hoechst 33342 double staining

According to instructions from the EdU Labeling/Detection Kit (Ribo-bio, Guangzhou, China), SCs ($2.5 \times 10^4/cm^2$) were plated onto 24-well plates and incubated in medium containing 10 μM EdU for 48 hours at 37°C under 5% CO_2. Subsequently, the SCs were fixed with 4% paraformaldehyde for 30 minutes. After rinsing with PBS, SCs were incubated with 200 μL of 1× Apollo® reaction cocktail per well at 37°C for 30 minutes, permeated with 0.2% Triton X-100 in PBS, and stained with Hoechst 33342 dye (5 g/mL) for 30 minutes. Images were observed under a fluorescence microscope (Olympus Imaging Systems). The percentage of EdU-positive cells was calculated using Image Pro Plus 5.0 software (Media Cybernetics, Silver Spring, MD, USA) in five random fields of three samples.

Flow cytometry of SC cycle

Cell cycle analysis was performed as previously described (Wang et al., 2009). After culturing in 6-well plates for 48 hours and reaching 90% confluency, SCs were trypsinized and resuspended at a cell density of 1×10^6 cells/mL. SCs were fixed in 70% cool ethanol overnight at –20°C. The fixed cells were incubated in tubes with 500 μL propidium iodide (50 μg/mL) for 1 hour in the dark at 4°C. The number of different cell cycle phases was detected using flow cytometry, and the results were analyzed with ModFitLT V3.0 software (Verity Software House, Topsham, ME, USA). The proliferative index was equal to the percentage of cells in the S and G_2M phases.

Real-time polymerase chain reaction (RT-PCR)

After SCs were cultured for 48 hours on non-coated or ECM-coated glass slides, total cellular RNA was extracted using TRIzol reagent (Invitrogen). The cDNA was synthesized from total RNA using a ReverTra Ace® qPCR RT Kit (Toyobo, Osaka, Japan) according to the supplier's instructions. The primer sequences for S100, glial fibrillary acidic protein (GFAP), P0, nerve growth factor (NGF), brain-derived neurotrophic factor (BDNF), glial cell line-derived neurotrophic factor (GDNF), vascular endothelial growth factor (VEGF), and glyceraldehyde-3-phosphate dehydrogenase (GAPDH) are shown in **Table 1**. The SYBR® Green Real-time PCR Master mix (Toyobo) was used to quantify mRNA expression ac-

cording to the manufacturer's instructions. Reaction mixtures were incubated at 95°C for 15 seconds (denaturation), 58°C for 15 seconds (annealing), and 72°C for 45 seconds (extension) for 40 cycles. The $2^{-\Delta\Delta Ct}$ method was used to analyze RT-PCR results. GAPDH was used as an endogenous control.

Western blot assay

SCs were cultured on non-coated or ECM-coated plates for 48 hours. Protein samples were separated using sodium dodecyl sulfate polyacrylamide gel electrophoresis, and then transferred onto polyvinylidene difluoride membranes and incubated with rabbit monoclonal antibody against NGF (1:500; Abcam), mouse monoclonal antibody against BDNF (1:200; Abcam), rabbit polyclonal antibody against GDNF (1:200; Abcam), and mouse monoclonal antibody against VEGF (1:200; Abcam) for 3 hours at 37°C. The membranes were incubated with horseradish peroxidase-conjugated secondary antibodies: goat anti-mouse IgG (1:4 000) and goat anti-rabbit IgG (1:4 000) for 1 hour at 37°C. The images were detected using a GS800 Densitometer Scanner (Bio-Rad, Hercules, CA, USA), and data were analyzed using PDQuest 7.2.0 software (Bio-Rad). β-Actin was used as an internal control. Results were reported as the gray value ratio of protein to β-actin.

DRG explant culture and immunofluorescence staining

Primary DRG neurons were cultured as previously described (de Luca et al., 2015). Briefly, DRGs were collected from newborn 12-hour-old Sprague-Dawley rats, digested twice in 0.125% (w/v) collagenase type IV (Sigma) for 1 hour, continually trypsinized using 0.25% (w/v) trypsin for 30 minutes, and mechanically dissociated in DMEM/F12 (Gibco) supplemented with 1% N_2 (Invitrogen) and 1% penicillin/streptomycin (Sigma). After centrifugation and resuspension, the cells were plated on non-coated (control group) or ECM-coated dishes (ECM group) at $5 \times 10^4/cm^2$. After 72 hours of incubation, the cells were fixed in 4% paraformaldehyde for 15 minutes and allowed to incubate with polyclonal antibody against neurofilament heavy (NF200; 1:200; Sigma) for 12 hours at –4°C, followed by incubation with secondary antibody (Alexa Fluor®594) for 1 hour in the dark at 37°C. Images were collected by fluorescence microscopy (Olympus). The neurite length of DRG neurons was calculated using Image Pro Plus 5.0 software (Media Cybernetics) from five random fields of three independent samples.

Statistical analysis

All quantitative data were expressed as the mean ± SD. Statistical analysis was performed using a two-sample *t*-test with the SPSS 17.0 software (SPSS, Chicago, IL, USA). A *P*-value < 0.05 was considered statistically significant.

Results

Biological characterization of hUCMSCs

Under a phase-contrast microscope, hUCMSCs at P4 appeared fibroblast-like in shape (**Figure 1A**). To determine hUCMSC multipotency, cells were cultured with three types of lineage-specific induction medium; adipogenic (**Figure 1B**), osteogenic (**Figure 1C**), and chondrogenic (**Figure 1D**) differentiations were determined using Oil-red O staining, Alizarin red staining, and Alcian blue staining, respectively. Image-based cytometry permitted quick visualization and instantaneous quantitative analysis of thousands of heterogeneous cells. The images revealed co-expression of CD73, CD90, and CD105 on the hUCMSC surface, as well as negative CD45 expression (**Figure 1E**). Quantitative analysis revealed that hUCMSCs expressed cell surface markers, including CD44 (98.1%), CD73 (99.1%), CD90 (99.6%), and CD105 (99.3%), although CD34 (0.04%, hematopoietic/endothelial marker) and CD45 (2.88%, hematopoietic marker) expression was negative (**Figure 1F**).

Morphology of hUCMSC-derived ECM

After stimulation with ascorbic acid for 7 days, hUCMSCs were embedded in secreted ECM and aligned in local fields under a phase-contrast microscope (**Figure 2A**) and scanning electron microscope (**Figure 2C**). After cell removal using a previous protocol, hUCMSC-derived ECM consisted of a large number of filaments homogeneously distributed into an aligned network by light microscopy (**Figure 2B**). Scanning electron microscopy images demonstrated the ECM fibrillary suprastructure, which was aligned and packed (**Figure 2D**, **E**). High magnification revealed an ultrastructure with 10–100-nm pores (**Figure 2F**).

ECM components

Immunofluorescence was used to identify the hUCMSC-derived ECM components, confirming that ECM was rich in laminin (**Figure 3A**), fibronectin (**Figure 3B**), collagen I (**Figure 3D**), collagen IV (**Figure 3E**), and collagen X (**Figure 3G**), which play important roles in peripheral nerve regeneration.

Table 1 Primers used for real-time polymerase chain reaction analysis

Gene	Forward primer (5′–3′)	Product size (bp)
GAPDH	Forward: ATG GTG AAG GTC GGT GTG AAC G Reverse: TTA CTC CTT GGA GGC CAT GTA G	21
S100	Forward: ATG TCT GAG CTG GAG AAG G Reverse: TCA CTC ATG TTC AAA GAA CTC	23
GFAP	Forward: GGA CAT CGA GAT CGC CAC CTA CAG Reverse: CAT CCC GCA TCT CCA CCG TCT TTA C	24
P0	Forward: GCT CTT CTC TTC TTT GGT GCT GTC C Reverse: GGC GTC TGC CGC CCG CGC TTC G	22
NGF	Forward: ATG TCC ATG TTG TTC TAC AC Reverse: TCA GCC TCT CTT GCA GCC C	19
BDNF	Forward: ATG ACC ATC CTT TTC CTT AC Reverse: CTA TCT TCC CCT TTT AAT GG	19
GDNF	Forward: GAA CCA AGC CAG TGT ATC TCC T Reverse: ATC GTC TCT GCC TTT GTC CTC	20
VEGF	Forward: ATG ATG AAG CCC TGG AGT GC Reverse: TGG TGG TGT GGT GGT GAC AT	20

GAPDH: Glyceraldehyde-3-phosphate dehydrogenase; GFAP: glial fibrillary acidic protein; NGF: nerve growth factor; BDNF: brain-derived neurotrophic factor; GDNF: glial cell-derived neurotrophic factor; VEGF: vascular endothelial growth factor.
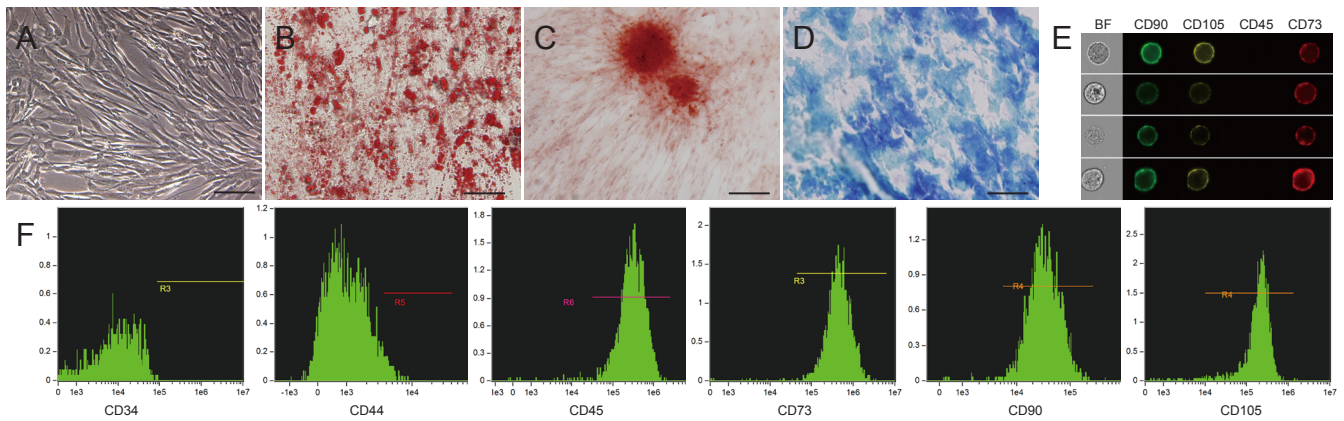
Figure 1 Biological characterization of hUCMSCs.
(A) Phase-contrast microscopy image of hUCMSCs at passage 4. (B–D) Results of trilineage differentiation of hUCMSCs, which can differentiate into adipogenic (B, Oil-red O staining), osteogenic (C, Alizarin red staining), and chondrogenic lineages (D, Alcian blue staining). Scale bars in A–D: 100 μm. (E) Image-based cytometry images showed co-expression of CD73 (red), CD90 (green), and CD105 (yellow) on the surface of hUCMSCs, as well as negative CD45 expressions. (F) Image-based cytometry showed positive expression for CD44, CD73, CD90, and CD105, and negative expression for CD34 and CD45. hUCMSCs: Human umbilical cord-derived mesenchymal stem cells.
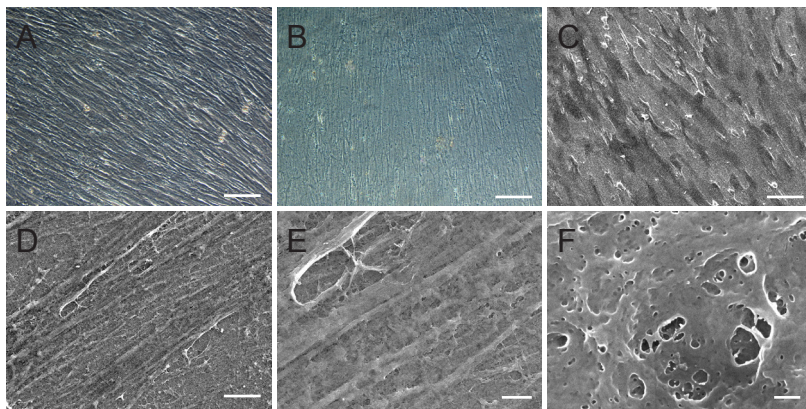
Figure 2 Morphology of hUCMSC-derived ECM.
(A) Phase-contrast microscopy image and (C) scanning electron microscopy image of hUCMSC-derived ECM before decellularization. (B) Phase-contrast microscopy image and (D) scanning electron microscopy image of hUCMSC-derived ECM after decellularization. (E) Higher magnification of the dotted area in D. (F) Higher magnification of the dotted area in E. Scale bars: A–C, 100 μm; D, 10 μm; E, 2 μm; F, 200 nm. ECM: Extracellular matrix; hUCMSCs: human umbilical cord-derived mesenchymal stem cells.
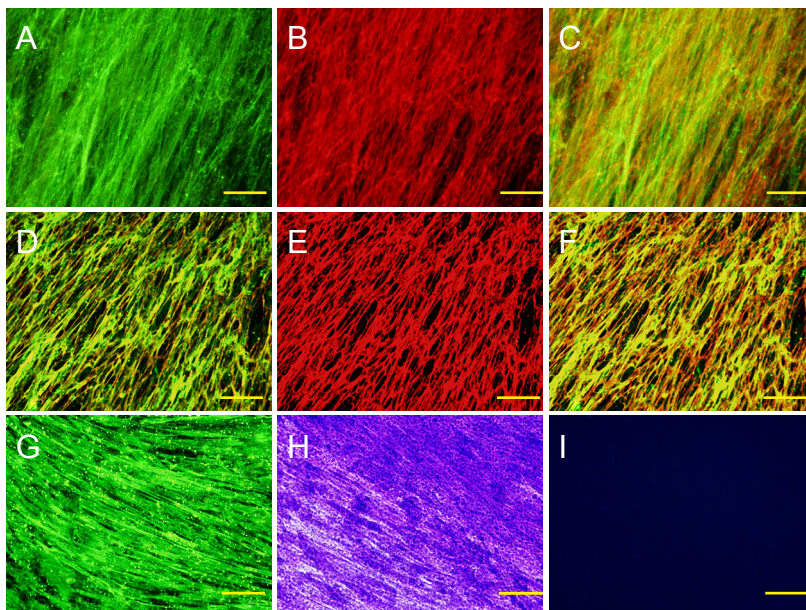
Figure 3 Components of hUCMSC-derived ECM.
(A–C) Laminin (green, A) and fibronectin (red, B) immunofluorescence of hUCMSC-derived ECM and their merged image (C). (D–F) Collagen I (green, D) and collagen IV (red, E) immunofluorescence of hUCMSC-derived ECM and their merged image (F). (G) Collagen X (green) immunofluorescence of hUCMSC-derived ECM. (H) Alcian blue staining of hUCMSC-derived ECM. (I) Hoechst 33258 staining of hUCMSC-derived ECM. Scale bars: 100 μm. ECM: Extracellular matrix; hUCMSC: human umbilical cord-derived mesenchymal stem cell.

The toluidine blue staining revealed that a large number of glycosaminoglycans, which regulate cell adhesion, were bound to the ECM surface. Hoechst 33258 staining showed a complete decellularization process.

Effects of hUCMSC-derived ECM on rat SC culture
Rat SCs were cultured on non-coated or ECM-coated glass slides for 48 hours. S100 and laminin immunohistochemistry showed SC adhesion and morphology on hUCMSC-de-
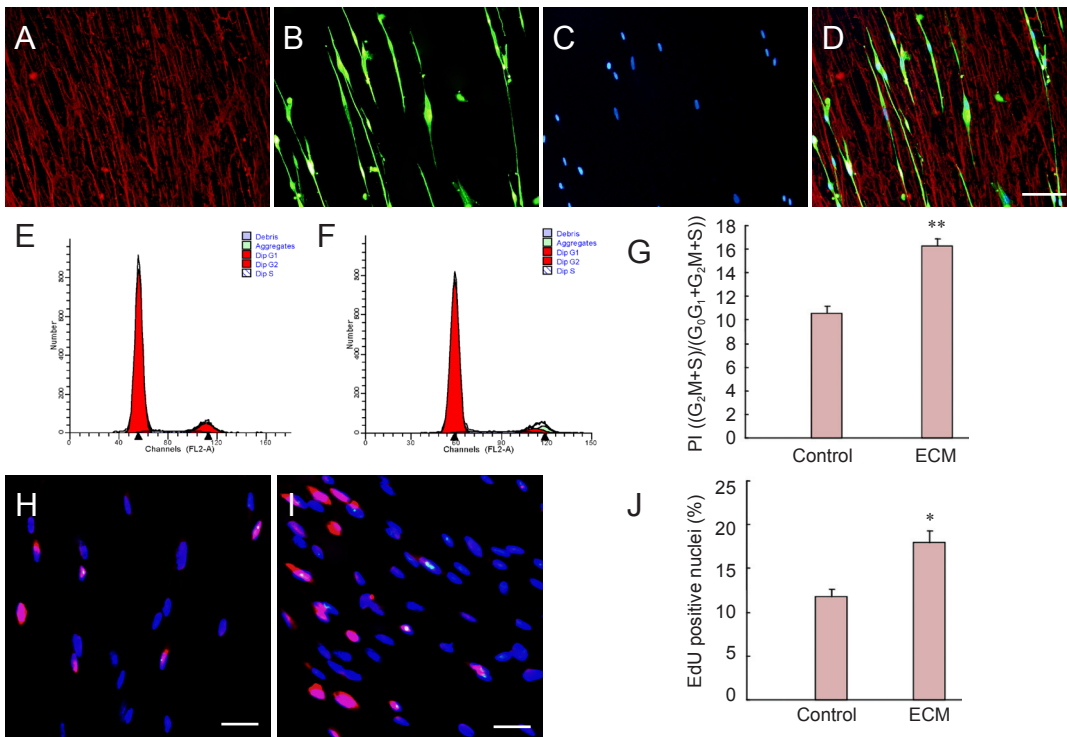
Figure 4 hUCMSC-derived ECM promotes proliferation of rat Schwann cells.
(A–D) S100 (green) and laminin (red) immunochemistry shows Schwann cell adhesion and morphology on hUCMSC-derived ECM. Scale bar: 100 μm. (E, F) Cell cycle analyzed by flow cytometry. (G) Comparison of SC proliferative index between control group (H, plated on non-coated dishes) and ECM group (I, plated on ECM-coated dishes). (H, I) EdU (red)/Hoechst 33342 (blue) immunofluorescence in control and ECM groups. (J) Comparison of SC EdU-positive nuclei between control and ECM groups. Scale bars: 100 μm. *$P < 0.05$, **$P < 0.01$, *vs.* control group. Data are expressed as the mean ± SD. Statistical analysis was performed using two-sample *t*-test. ECM: Extracellular matrix; SCs: Schwann cells; hUCMSCs: human umbilical cord-derived mesenchymal stem cell; PI: proliferative index.
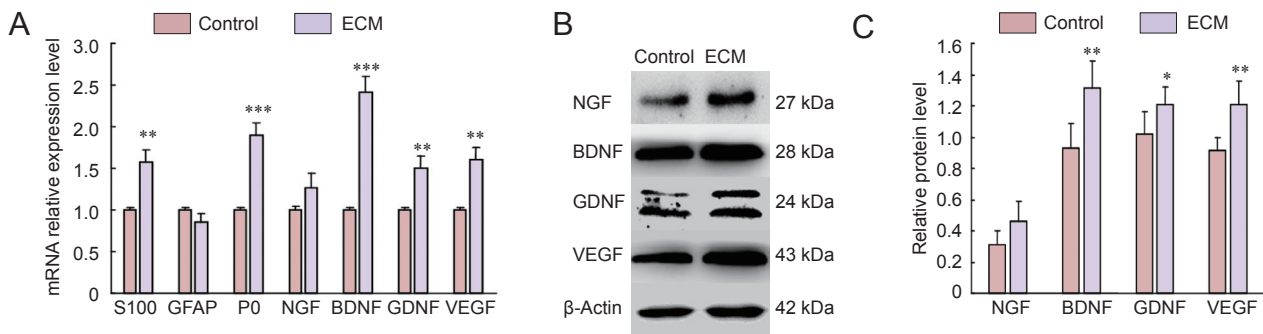
Figure 5 The mRNA and protein expression of related factors in control and ECM groups.
(A) The mRNA levels ($2^{-\Delta\Delta Ct}$) of S100, GFAP, P0, NGF, BDNF, GDNF, and VEGF in the control group (plated on non-coated dishes) and ECM group (plated on ECM-coated dishes). **$P < 0.01$, ***$P < 0.001$, *vs.* control group. (B, C) Protein levels (gray value: target proteins/β-actin) of NGF, BDNF, GDNF, and VEGF in control and ECM groups. *$P < 0.05$, **$P < 0.01$, *vs.* control group. Data are expressed as the mean ± SD. Statistical analysis was performed using two-sample *t*-test. ECM: Extracellular matrix; GFAP: glial fibrillary acidic protein; NGF: nerve growth factor; BDNF: brain-derived neurotrophic factor; GDNF: glial cell-derived neurotrophic factor; VEGF: vascular endothelial growth factor.
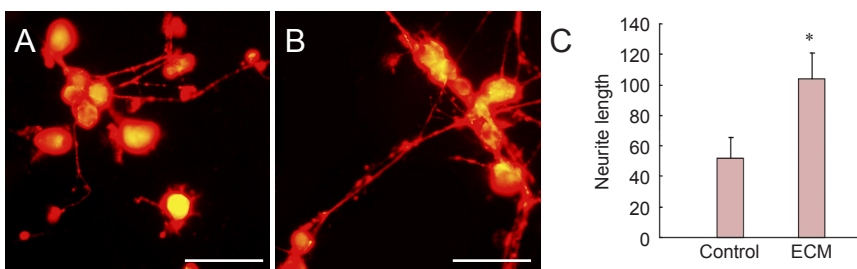
Figure 6 Effect of hUCMSC-derived ECM on rat DRG neurons.
(A, B) NF200 staining of DRG neurons in control group (A, plated on non-coated dishes) and ECM group (B, plated on ECM-coated dishes). Scale bars: 200 μm. (C) Semi-quantitative immunofluorescent analysis shows significantly longer neurite length of DRG neurons in the ECM group compared with the control group. *$P < 0.05$, *vs.* control group. Data are expressed as the mean ± SD. Statistical analysis was performed using two-sample *t*-test. ECM: Extracellular matrix; hUCMSCs: human umbilical cord-derived mesenchymal stem cells; DRG: dorsal root ganglion.

rived ECM (**Figure 4A–D**). SCs were bipolar according to the direction of ECM laminin and were aligned end to end. Flow cytometric analysis of the SC cycle indicated a significantly higher proliferative index in the ECM group than in the control group (16.28 ± 0.57% *vs.* 10.56 ± 0.58%, *P* < 0.01; **Figure 4E–G**). EdU (red)/Hoechst 33342 (blue) immunofluorescence results showed that ECM promoted SC proliferation (**Figure 4H–J**). The percentage of EdU-positive cells in the ECM group was significantly higher than in the control group (18.03 ± 1.30% *vs.* 11.80 ± 0.86%, *P* < 0.05; **Figure 4J**).

RT-PCR results indicated significantly increased mRNA levels of S100, P0, NGF, GDNF, and VEGF in SCs cultured on ECM-coated plates compared with SCs cultured on non-coated plates (*P* < 0.05; **Figure 5A**). Western blot assay results confirmed that SCs cultured on ECM-coated plates improved NGF, GDNF, and VEGF protein levels compared with SCs cultured on non-coated plates, although NGF showed no significant difference (*P* < 0.05; **Figure 5**, **C**).

Effect of hUCMSC-derived ECM on rat DRG neurons

Rat DRG neurons were cultured on non-coated or ECM-coated glass slides for 72 hours. Immunofluorescence showed a significantly greater neurite length of DRG neurons in the ECM group than in the control group (103.6 ± 17.22 μm *vs.* 52.01 ± 13.77 μm, *P* < 0.05; **Figure 6A–C**).

Discussion

Although considerable success has been achieved with individual ECM molecules and tissue-derived ECM in promoting peripheral nerve regeneration, several drawbacks still exist. Thus, the exploration of cell-derived ECM in peripheral nerve regeneration is warranted. In this study, hUCMSCs were used to fabricate cell-derived ECM. This idea was based on the hypothesis that a young decellularized ECM may promote proliferation and maintain the "stemness" of MSCs. Li et al. (2014) demonstrated that decellularized ECM deposited by fetal synovium-derived stem cells could rejuvenate human adult synovium-derived stem cells by promoting proliferation and chondrogenic potential. Apparently, ECM-derived fetal stem cells possess a superior proliferative capacity relative to ECM-derived adult stem cells. Moreover, hUCMSCs have several advantages, such as a painless collection procedure, faster self-renewal, and hypo-immunogenic properties; the cells are also less ethically problematic (Nagamura-Inoue and He, 2014). Therefore, we developed a protocol to prepare and characterize hUCMSC-derived ECM and investigated its function in peripheral nerve regeneration.

The key fabrication procedure in the hUCMSC-derived ECM is anchoring the ECM to the carrier and preventing matrix delamination when ECM is prepared by decellularization. In this study, we coated the glass slides with fibronectin (25 μg/mL) for 1 hour at 37°C. The immobilized fibronectin monolayer anchored the ECM molecules *via* its binding domains with collagens, heparins, fibrin, and fibronectin. Furthermore, fibronectin covalently binds to the glass surface *via* reactive copolymer thin-film chemistry to enhance stabilization. Compared with tropocollagen, fibrillary collagen, and poly-L-lysine, Prewitz et al. (2013) found

that fibronectin generates a superior ECM.

In the present study, topology of the hUCMSC-derived ECM was observed using light and electron micrography. Results showed that hUCMSCs tended to grow with a spontaneous orientation. After decellularization, the hUCMSCs easily aligned to form the ECM. Based on this phenomenon, we hypothesized that the growth orientation could be controlled using physicochemical technology to build an aligned ECM. With electron micrography at high magnification, ECM exhibited a three-dimensional structure with a large number of micropores, which may facilitate the cell-matrix interaction. The topology provided a basis to modify a neural conduit with hUCMSC-derived ECM.

The different proteins in our hUCMSC-derived ECM detected by immunofluorescence revealed that the ECM could provide a suitable niche for peripheral nerve regeneration. ECM proteins were previously considered to be MSC and hematopoietic stem/progenitor cell niche regulators (Dellatore et al., 2008). However, the primary ECM components, such as collagens, laminin, and fibronectin, also play crucial roles in peripheral nerve repair. Collagens are a group of glycoproteins that provide structural guidance and store growth factors. The main subfamilies include fibril-forming collagens (types I, II, III, V), networking collagens (IV, VI, VIII, X), and other collagens (Byron et al., 2013; Gonzalez-Perez et al., 2013). We focused on collagen type I because of its association with fibril formation, as well as on collagen type IV because of its association with the basement membrane in the peripheral nervous system. Among the ECM non-collagenous glycoprotein molecules, the most important are laminins and fibronectins. Laminins participate in cell proliferation, adhesion, migration, and differentiation activities (Plantman, 2013; Lin et al., 2014). Moreover, laminin is an essential component for SC differentiation, axon myelination, and regeneration in peripheral nerves (Chen and Strickland, 2003; Yu et al., 2009). Fibronectin is the other major ECM component; it increases outgrowth from several types of neurons, such as embryonic DRG neurons, sympathetic ganglions, and spinal cord neurons (Rogers et al., 1983; Gardiner et al., 2007). Fibronectin also forms a fibrillary matrix and supports cell binding and cell migration. In brief, the hUCMSC-derived ECM molecules, such as laminins, fibronectin, collagens, nidogens, thrombospondins, and vitronectin, present an orchestrated niche for peripheral nerve regeneration.

Cultures of SCs and DRG neurons on the surface of the hUCMSC-derived ECM demonstrated that the ECM promotes SC proliferation and neurite growth. This may be attributed to the cell-matrix interaction, which induces cell signaling transmission from both laminins and fibronectins (Pei et al., 2011). The integrins, a major ECM receptor, mediate the biological process and regulate cell survival, proliferation, differentiation, and matrix remodeling (Loeser, 2002). Results from the present study will help to create a novel three-dimensional expansion system for SCs and DRG neurons to mimic the peripheral nerve regenerative niche. Structurally, the niche is formed by supported cells and a matrix. However, an accurate definition of the precise cellular components and anatomical structure of the niche remains challenging.

Conversely, RT-PCR and western blot assay revealed that hUCMSC-derived ECM promotes expression of neurotrophic factors (NGF, BDNF, and GDNF) and angiogenesis factors (VEGF) in SCs. These growth factors play important roles in SC proliferation, neuronal neurite regrowth, and new blood vessel regeneration. Our findings indicated that hUCMSC-derived ECM enhances the paracrine function of endogenous SCs. Additionally, a cell-derived ECM can promote proliferation and maintain stemness of exogenous stem cells (Xiong et al., 2015; Zhang et al., 2015), indicating that cell-derived ECM also helps to build an appropriate niche for transplanted stem cells. We also hypothesized that cell-derived ECM may synergize the paracrine effect of exogenous stem cells, which requires further investigation.

In summary, a hUCMSC-derived ECM builds a novel three-dimensional expansion system for SCs and DRG neurons to mimic the peripheral nerve regeneration niche. Based on our results, the ECM promotes SC proliferation and neurite growth. The ECM influences peripheral nerve regeneration *via* three modes: (1) three-dimensional structure and different components for cell adhesion and proliferation; (2) intracellular signaling activated by cell-matrix interactions; and (3) regulation of the paracrine function of endogenous SCs. However, further research is needed to determine the mechanisms of ECM involved in peripheral nerve regeneration.

References

Armstrong SJ, Wiberg M, Terenghi G, Kingham PJ (2007) ECM molecules mediate both Schwann cell proliferation and activation to enhance neurite outgrowth. Tissue Eng 13:2863-2870.

Brown JM, Shah MN, Mackinnon SE (2009) Distal nerve transfers: a biology-based rationale. Neurosurg Focus 26:E12.

Byron A, Humphries JD, Humphries MJ (2013) Defining the extracellular matrix using proteomics. Int J Exp Pathol 94:75-92.

Chen XD, Dusevich V, Feng JQ, Manolagas SC, Jilka RL (2007) Extracellular matrix made by bone marrow cells facilitates expansion of marrow-derived mesenchymal progenitor cells and prevents their differentiation into osteoblasts. J Bone Miner Res 22:1943-1956.

Chen ZL, Strickland S (2003) Laminin gamma1 is critical for Schwann cell differentiation, axon myelination, and regeneration in the peripheral nerve. J Cell Biol 163:889-899.

de Luca AC, Faroni A, Reid AJ (2015) Dorsal root ganglia neurons and differentiated adipose-derived stem cells: an in vitro co-culture model to study peripheral nerve regeneration. J Vis Exp. DOI: 10.3791/52543.

Dellatore SM, Garcia AS, Miller WM (2008) Mimicking stem cell niches to increase stem cell expansion. Curr Opin Biotechnol 19:534-540.

Gao X, Wang Y, Chen J, Peng J (2013) The role of peripheral nerve ECM components in the tissue engineering nerve construction. Rev Neurosci 24:443-453.

Gardiner NJ, Moffatt S, Fernyhough P, Humphries MJ, Streuli CH, Tomlinson DR (2007) Preconditioning injury-induced neurite outgrowth of adult rat sensory neurons on fibronectin is mediated by mobilisation of axonal alpha5 integrin. Mol Cell Neurosci 35:249-260.

Gonzalez-Perez F, Udina E, Navarro X (2013) Extracellular matrix components in peripheral nerve regeneration. Int Rev Neurobiol 108:257-275.

Gould LJ (2016) Topical Collagen-Based Biomaterials for Chronic Wounds: Rationale and Clinical Application. Adv Wound Care (New Rochelle) 5:19-31.

Gu Y, Ji Y, Zhao Y, Liu Y, Ding F, Gu X, Yang Y (2012) The influence of substrate stiffness on the behavior and functions of Schwann cells in culture. Biomaterials 33:6672-6681.

Gu Y, Zhu J, Xue C, Li Z, Ding F, Yang Y, Gu X (2014) Chitosan/silk fibroin-based, Schwann cell-derived extracellular matrix-modified scaffolds for bridging rat sciatic nerve gaps. Biomaterials 35:2253-2263.

Hoshiba T, Chen G, Endo C, Maruyama H, Wakui M, Nemoto E, Kawazoe N, Tanaka M (2016) Decellularized extracellular matrix as an in vitro model to study the comprehensive roles of the ECM in stem cell differentiation. Stem Cells Int 2016:6397820.

Li J, Hansen KC, Zhang Y, Dong C, Dinu CZ, Dzieciatkowska M, Pei M (2014) Rejuvenation of chondrogenic potential in a young stem cell microenvironment. Biomaterials 35:642-653.

Lin CY, Li LT, Su WT (2014) Three dimensional chitosan scaffolds influence the extra cellular matrix expression in Schwann cells. Mater Sci Eng C Mater Biol Appl 42:474-478.

Loeser RF (2002) Integrins and cell signaling in chondrocytes. Biorheology 39:119-124.

Nagamura-Inoue T, He H (2014) Umbilical cord-derived mesenchymal stem cells: Their advantages and potential clinical utility. World J Stem Cells 6:195-202.

Pei M, Li JT, Shoukry M, Zhang Y (2011) A review of decellularized stem cell matrix: a novel cell expansion system for cartilage tissue engineering. Eur Cell Mater 22:333-343.

Peng J, Wang Y, Zhang L, Zhao B, Zhao Z, Chen J, Guo Q, Liu S, Sui X, Xu W, Lu S (2011) Human umbilical cord Wharton's jelly-derived mesenchymal stem cells differentiate into a Schwann-cell phenotype and promote neurite outgrowth in vitro. Brain Res Bull 84:235-243.

Plantman S (2013) Proregenerative properties of ECM molecules. Biomed Res Int 2013:981695.

Prewitz MC, Seib FP, von Bonin M, Friedrichs J, Stissel A, Niehage C, Muller K, Anastassiadis K, Waskow C, Hoflack B, Bornhauser M, Werner C (2013) Tightly anchored tissue-mimetic matrices as instructive stem cell microenvironments. Nat Methods 10:788-794.

Rogers SL, Letourneau PC, Palm SL, McCarthy J, Furcht LT (1983) Neurite extension by peripheral and central nervous system neurons in response to substratum-bound fibronectin and laminin. Dev Biol 98:212-220.

Wang J, Ding F, Gu Y, Liu J, Gu X (2009) Bone marrow mesenchymal stem cells promote cell proliferation and neurotrophic function of Schwann cells in vitro and in vivo. Brain Res 1262:7-15.

Wang Y, Zhao Z, Ren Z, Zhao B, Zhang L, Chen J, Xu W, Lu S, Zhao Q, Peng J (2012) Recellularized nerve allografts with differentiated mesenchymal stem cells promote peripheral nerve regeneration. Neurosci Lett 514:96-101.

Xiong Y, He J, Zhang W, Zhou G, Cao Y, Liu W (2015) Retention of the stemness of mouse adipose-derived stem cells by their expansion on human bone marrow stromal cell-derived extracellular matrix. Tissue Eng Part A 21:1886-1894.

Yu WM, Chen ZL, North AJ, Strickland S (2009) Laminin is required for Schwann cell morphogenesis. J Cell Sci 122:929-936.

Zhang W, Zhu Y, Li J, Guo Q, Peng J, Liu S, Yang J, Wang Y (2016) Cell-derived extracellular matrix: basic characteristics and current applications in orthopedic tissue engineering. Tissue Eng Part B Rev doi:10.1089/ten.TEB.2015.0290.

Zhang Z, Luo X, Xu H, Wang L, Jin X, Chen R, Ren X, Lu Y, Fu M, Huang Y, He J, Fan Z (2015) Bone marrow stromal cell-derived extracellular matrix promotes osteogenesis of adipose-derived stem cells. Cell Biol Int 39:291-299.